Mimicking cell/extracellular matrix adhesion with lipid membranes and solid substrates: requirements, pitfalls and proposals

2004 J. Phys.: Condens. Matter 16 S2427

(http://iopscience.iop.org/0953-8984/16/26/016)

INSTITUTE OF PHYSICS PUBLISHING JOURNAL OF PHYSICS: CONDENSED MATTER

J. Phys.: Condens. Matter **16** (2004) S2427–S2437 PII: S0953-8984(04)72553-9

Mimicking cell/extracellular matrix adhesion with lipid membranes and solid substrates: requirements, pitfalls and proposals

Damien Cuvelier[1], **Cyrille Vezy**[2], **Annie Viallat**[2], **Patricia Bassereau**[1] **and Pierre Nassoy**[1,3]

[1] Laboratoire de Physico-Chimie Curie, UMR 168 (CNRS)—Institut Curie, 75005 Paris, France
[2] Laboratoire de Spectrométrie Physique, UMR C5588 (CNRS)—Université Joseph Fourier, 38402 Saint Martin d'Hères, France

E-mail: pierre.nassoy@curie.fr

Received 25 November 2003
Published 18 June 2004
Online at stacks.iop.org/JPhysCM/16/S2427
doi:10.1088/0953-8984/16/26/016

Abstract

The interest in physical approaches to the study of cell adhesion has generated numerous recent works on the development of substrates mimicking the extracellular matrix and the use of giant synthetic liposomes, commonly considered as basic models of living cells. The use of well-characterized bioactive substrates and artificial cells should allow us to gain new insight into the cell–extracellular matrix interactions, provided that their biomimetic relevance has been really proved. The aim of this paper is to define some minimal requirements for effective biomimetic features and to propose simple adhesion assays. We show, for instance, that immobilization of specific ligands is sometimes not sufficient to ensure specific adhesion of cells expressing the corresponding receptors. By investigating comparatively the adhesive behaviour of decorated erythrocytes and vesicles, we also discuss the potentialities and limitations of synthetic vesicles as test cells.

1. Introduction

Cell adhesion to the extracellular matrix (ECM) is primarily mediated by transmembrane proteins called cell adhesion molecules (CAMs), which involve specific interactions and allow cells to adhere only to other cells that express the appropriate receptors. Although cascades of intracellular signalling events are triggered upon cell adhesion, it is now well accepted that the degree of refinement of bioadhesion (at least in the early stages) can be partly attributed to the sophisticated molecular structure of the cell surface, which is composed of a lipid membrane

[3] Author to whom any correspondence should be addressed.

and a variety of CAMs embedded in a glycopolymer brush called glycocalix [1]. From the viewpoint of physicists, experiments on real living cells are difficult to interpret because (i) usually more than one CAM participates in adhesion, (ii) the expression level of surface proteins varies drastically over time and (iii) adhesion patches are likely to be reinforced or weakened upon reorganization of the cell cytoskeletal structure [2].

To understand the physical basis of cell adhesion, it is therefore crucial to design biomimetic systems for both ECM and cells. Over the last three decades, many proposals for artificial extracellular matrices and mimics of cells have been developed [3, 4]. Although a plethora of reports were successful in immobilizing biological ligands on solids or lipid bilayers, very few could really pretend to achieve some mimetic properties for bioadhesion. One has indeed to keep in mind that the high degree of specific recognition required by cell adhesion and its reversibility implicitly mean that generic attractions (e.g. van der Waals, electrostatic) are almost completely inhibited in cell–cell interactions. The principal challenge in all biomimetic attempts is therefore to allow molecular recognition between surface ligands and receptors while preventing non-specific interactions between the cell membrane and the biomaterial. The aim of the present paper is to define the minimal design requirements in terms of substrate modification and synthetic cell preparation in order to emulate the adhesion of cells to the ECM in a realistic manner.

The most straightforward approach for preparing supposedly biomimetic substrates has consisted in adsorbing a solution of matrix proteins onto solid surfaces. This method was, however, shown to be not satisfactory, because proteins often undergo denaturation at the interface [5]. Consequently, a fraction of immobilized ligands is inactive, or more importantly, is likely to generate undesired generic attractions. More recently, novel strategies based on a finer control of the surface chemistry have been developed [6, 7]. However, the development of more complex approaches to design decorated surfaces and membranes has not systematically been tested in a biomimetic perspective.

In section 1, we will point out some common pitfalls to avoid and suggest adhesion assays to perform if one wants to test the biomimetic relevance of artificial ECM. In particular, we will show that molecular recognition between immobilized ligands and soluble receptors is not always a guarantee for specific cellular recognition. In section 2, we will propose a simple strategy of ligand immobilization, which will be shown to meet the minimal requirements for specific bioadhesion. Finally, section 3 will be dedicated to the design of cell mimics based on the use of giant synthetic vesicles. A comparison between red blood cells and vesicles will be pursued. Whereas most of the static features of adhesion are found to be similar, we will insist on some limitations in the mimicry of the dynamics of spreading.

2. Experimental details

Substrates

Glass coverslides were selected as templates. All glass surfaces were first activated with an amino-terminated silanizing agent (*N*-[3-(trimethoxysilyl)propyl]ethylenediamine from Sigma-Aldrich) following a procedure described elsewhere [8]. As a model receptor–ligand pair, we chose the biotin–streptavidin complex, which is known to be very stable, and can serve to produce universal templates for further immobilization of any kind of biotinylated protein. Our strategies to tailor surfaces with biotin involved either adsorption of biotin-derivatized proteins or grafting of various biotinylated crosslinkers. More precisely, bovine serum albumin (BSA) and β-casein (Sigma-Aldrich) were tagged with sulfo-NHS-biotin (Pierce) following standard protocols [3]. Over the timescale of our experiments ($<$1 h), adsorption of BSA

and casein could be considered as irreversible [5]. Alternatively, two biotinylated crosslinkers were used for covalent grafting. EZ-link-LC-LC-biotin (Pierce) and SBA-PEG^{3400}-biotin (Nektar) have the same amino-reactive group, namely *N*-hydroxysuccinimidyl, but differ in the structure of the spacer; the first one is composed of an 11-carbon alkyl chain while the second compound has a longer flexible chain made of 78 ethylene glycol units. Reaction of both crosslinkers to amino-silanized slides was performed in carbonate–bicarbonate buffer (pH 8.5). Controls for non-specific adhesion were obtained by using the non-biotinylated versions of the above-mentioned proteins and crosslinkers, meaning raw BSA and casein and SBA-PEG^{5000}-methoxy (Nektar). Finally, we also designed microstructured adherent/repellent surfaces by using the capillary reactive method described elsewhere [9]. Briefly, soft elastomeric moulds with the desired micrometre-sized relief features were fabricated by soft lithography [10] and the channels (straight, with curved portions or step-like) were transversally cut at both ends to open a path for incoming liquids. In the method based on the adsorption of casein, native casein was first transferred from the pre-inked stamp to the surface by microcontact printing. Then, before peeling the pad off, biotin–casein was injected by capillarity into the channels. In the method based on the grafting of PEG, a different strategy was used: biotin-PEG was first grafted inside the channels. In a second step, after removing the pad, the rest of the surface was passivated by grafting methoxy-PEG.

Vesicles and cells

Vesicles were prepared by electroformation [11] in 180 mOsm sucrose from a 95:4.5:0.5 mixture of egg phosphatidylcholin (EPC), 1,2-diacyl-*sn*-glycero-3-phosphoethanolamine-*N*-[methoxy(polyethylene glycol)-2000] (mPEG^{2000}-PE) and 1,2-distearoyl-*sn*-glycero-3-phosphoethanolamine-*N*-[biotinyl(polyethylene glycol)2000] (DSPE-PEG^{2000}-biotin). All the lipids were purchased from Avanti Polar Lipids. The presence of the PEG-lipid in the membrane creates a mobile polymer brush, which has been widely used to model the glycocalix [12]. The biotinylated lipids provide anchoring sites for streptavidin immobilization. The vesicles were finally coated with fluorescent streptavidin (Cy3-Extravidin from Sigma-Aldrich) by incubation and repeated gentle centrifugation (500 rpm for 5 min) to remove any free streptavidin. In order to test the relevance of these synthetic vesicles as mimics of cells, we compared their adhesive behaviour with that of osmotically swollen red blood cells (PBS 138 mOsm), which were preliminarily biotin-labelled according to a protocol described in [8] and streptavidin-coated by incubation in a solution of streptavidin.

Microscopy

Observation chambers were made of one biotinylated coverslip and one glass slide assembled using a parafilm spacer (100 μm thick). The chamber was filled with a suspension of vesicles or red blood cells and placed on the stage of an inverted microscope (Axiovert 200, Zeiss). Optical inspection of vesicles and red blood cells in contact with the substrate was performed by the combination of two methods:

(1) reflection interference contrast microscopy (RICM), which is a suitable interferometric technique to visualize adhesion patches or zones of intimate contact of cell membranes with flat substrates [13];
(2) epifluorescence microscopy, which allows us to map the concentration of fluorescent streptavidin molecules.

The microscope was equipped with optical filters, a 100× Plan-Achromat immersion oil objective (numerical aperture (NA) 1.4) and a CCD monochrome camera cooled to −30 °C

(Coolsnap HQ, Roper Scientific). All images were captured and analysed with software provided with the camera (MetaVue, Universal Imaging Corp.). Additionally, side-view images of vesicles were obtained by light microscopy using a 90° tipped microscope working at low-angle incidence [14].

3. Results and discussion

The specificity of cell–matrix recognition lies in the interplay between electrosteric plus undulation repulsions and receptor–ligand attractions [12, 15]. One of the key issues in the design of biomimetic systems consists in immobilizing the biomolecules of interest in their active conformations while inhibiting all kinds of generic long-range attractions. Some strategies of ligand immobilization will be discussed in detail (sections 1 and 2). Then, the potentiality for decorated vesicles to emulate simple cells like erythrocytes will be investigated (section 3). For the sake of simplicity, we restricted our study to a unique receptor–ligand model system, namely the streptavidin–biotin complex.

3.1. Immobilization of specific adhesion molecules does not ensure specific cell adhesion

Numerous chemical procedures have been developed to immobilize biotin and/or streptavidin on solid surfaces. They may involve various degrees of sophistication and complexity: from the adsorption of biotinylated proteins [16] to the use of self-assembled monolayers of biotin-terminated thiols on gold [17] or the design of supported bilayers containing biotinylated lipids [4]. The most common way to characterize the efficiency of immobilization is to test the capability of the biotinylated substrate to capture streptavidin (e.g. by fluorescence microscopy or AFM) [18]. Successful immobilization of streptavidin on a biotinylated surface often means that specific recognition has been achieved at the molecular scale. However, in order to obtain specific cellular recognition, one further needs to check that streptavidin-decorated cells specifically adhere to these biotinylated surfaces.

The first type of substrate that we have worked with was prepared by crosslinking the EZlink-LC-LC-biotin to an amino-silanized slide. Biotin immobilization was characterized by fluorescence intensity measurements. Signal-to-noise ratio was calculated by comparing the densities of fluorescence intensity after incubation with Cy3-Extravidin and with Cy3-Extravidin neutralized by free d-biotin. Typical values of 3.6 ± 0.5 were obtained for the S/N ratio, which suggests that molecules of streptavidin are efficiently and specifically captured. The specificity of cellular adhesion was then probed by seeding streptavidin-coated red blood cells onto substrates derivatized with LC-LC-biotin. Figure 1(a) shows a RICM image of a streptavidin-decorated swollen erythrocyte in contact with the slide in a protein-free buffer (PBS + diol-PEG3400 in order to avoid crenation of the cells). All red blood cells were fully spread, as revealed by contact area diameters of the order of the erythrocyte size (dark spot in RICM). Figures 1(b) and (c) correspond to two control experiments. Quite surprisingly, native erythrocytes exhibited similar RICM patterns with large contact patches (figure 1(b)). In contrast, when BSA was added to the cell suspension, areas of tight contact between cells and the substrate were much smaller than the projected area of the cell, typically limited to a few μm^2 (figure 1(c)) and cells could be easily detached under gentle flow. Obviously, we may conclude that adhesion of streptavidin-coated erythrocytes on LC-LC-biotin slides is not purely specific since (i) native cells equally well adhered to the substrate and (ii) addition of BSA inhibits adhesion, which suggests that LC-LC-biotin chemical treatment does not prevent adsorption of BSA on top of the biotin layer.

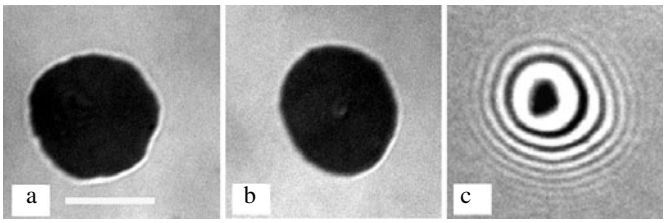

Figure 1. Adhesion assay on a glass slide modified with LC-LC-biotin (biotinylated crosslinker with a short aliphatic spacer). RICM images of: (a) a streptavidin-coated red blood cell in PBS; (b) a native red blood cell in PBS; (c) a streptavidin-coated red blood cell in PBS + 0.1% BSA. The bar length is 5 μm.

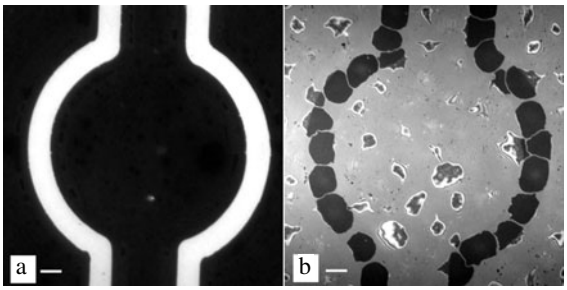

Figure 2. (a) Fluorescence micrographs of micropatterned surfaces. Stripes are functionalized with PEG-biotin and revealed by Cy3-Extravidin. Surrounding areas are passivated with methoxy-PEG. (b) RICM micrographs of streptavidin-coated erythrocytes seeded onto biotinylated patterned surfaces. Adhered red blood cells are co-localized with the biotin lines. Each bar is 5 μm in length.

3.2. Bio-activation and -passivation of surfaces

The outcomes of the experiments described above led us to define a few basic requirements to ensure specific cell recognition. It is of primary importance (1) to inhibit all generic interactions between cells and surface and (2) to avoid any adsorption of protein that could mask the bioactive sites. Passivation of surfaces against cell adhesion and protein adsorption can be achieved either by coating the surface with inert proteins, like casein (which is well known to act as a blocking agent in biology), or by grafting some derivatives of poly(ethylene glycol) [19]. Our strategy was thus to treat surfaces with biotin-derivatized casein or PEG. Doing so, the resulting surfaces are expected to present the dual features of both a passive layer that resists non-specifics and of a bioactive layer that specifically 'attracts' cells.

In order to test the possible higher efficiency of this approach, we designed micropatterned surfaces on which casein–biotin (respectively PEG-biotin) adhesive lines are separated by large passive areas covered by casein (respectively methoxy-PEG). The width of the stripe was chosen in the 4–7 μm range. Figure 2(a) displays a fluorescence photograph of the patterns obtained revealed by Cy3-Extravidin. For both kinds of substrates, S/N ratios were in the 8–11 range, which suggests that adsorption of streptavidin was strongly inhibited on the casein or PEG regions. Streptavidin-decorated erythrocytes were then selected as test cells for adhesion assays. The photograph in figure 2(b) was taken by RICM after seeding modified erythrocytes on the micropatterned surfaces. We observed that red blood cells with large contact areas were found along stripes that correspond to the biotinylated patterns. In contrast, blood cells weakly adhered to the surrounding passive areas.

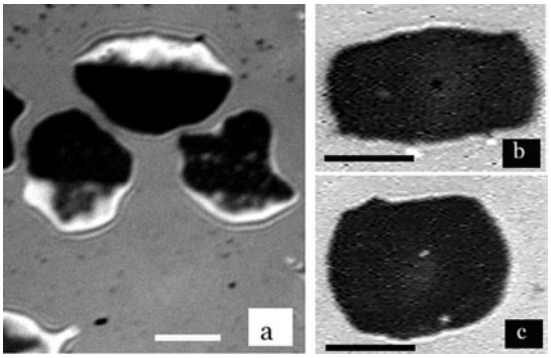

Figure 3. (a) Enlargement of a RICM image at the border between a biotinylated line and a passivated area. Red blood cells overlap the two regions but only adhere specifically to the biotin-grafted zone; (b) and (c) RICM micrographs of individual streptavidin-coated erythrocytes deformed along biotin stripes of respective widths 5 and 6.5 μm. Each bar length is 5 μm.

The enlargements in figure 3 focus on the main two adhesion patterns that were found. If a cell sediments on the border between an adherent stripe and a passivated area, it only partially adheres to the substrate. Within one cell, the contact area clearly stopped at the border (figure 3(a)). Since a red blood cell is not motile, it cannot move towards the adherent zone. Yet, without mentioning any active motion, we might also expect that the cell could simply roll towards the region of higher surface energy, in the same manner that a water droplet is pushed towards hydrophilic areas due to the non-compensated Young force between the rear and front of the drop [20]. We have never observed such a phenomenon. This may be rationalized if the contact between the cell and the substrate is almost irreversible, which is indeed the case on the timescale of the experiment ($\sim$30 min).

Micrographs (b) and (c) in figure 3 show how an individual streptavidin-coated erythrocyte gets deformed in contact with a biotinylated line. Both photographs correspond to two different widths of the adherent stripe. We observe that the width of the adhesion patch is strictly fixed by the width of the stripe, the cell being stretched along the line. Moreover, one may notice that the wider the line the smaller the axial deformation of the cell. To propose a rigorous mechanical model of cell deformation upon adhesion on micropatterned surfaces is outside the scope of the present paper. Nevertheless, we use semiquantitative arguments for the previous observation based on the theoretical analysis of the deformation of spherical cells performed by Parker and Winlove [21]. The authors have computed the force applied to the poles of spherical cells as a function of the polar strain.

Let us recall the main outcomes.

(1) The relevant dimensionless parameter is $C = a^2H/B$, where B is the out-of-plane stiffness, H is the in-plane shear modulus and a is the radius of the sphere;
(2) If C is large (typically >10), the force is directly proportional to the fractional extension, $\varepsilon = L/2a - 1$ (L is the length of the cell along the line) and is given by $F = 5\varepsilon(aBH^2)^{1/3}$.

Taking the literature values of $50k_BT = 2 \times 10^{-19}$ N m for B and 2×10^{-4} N m^{-1} for H [22], and $a = 3.5$ μm as the contact radius of a swollen streptavidin-coated erythrocyte on a surface fully covered with biotin, we check that $C = 12\,000 > 10$ and find that the extension force is given by $F = 150\varepsilon$ (pN). Since the cell is stretched because of spreading, F can also be crudely estimated by $F = W/b = \pi a^2 w/b$, where W is the adhesion energy, b is the stripe width and w is the adhesion energy per unit area. Assembling these two expressions

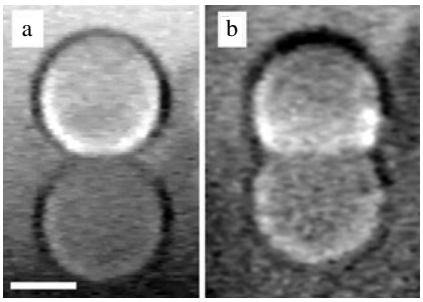

Figure 4. Side-view images of a streptavidin-decorated vesicle on: (a) an inert casein-coated substrate; (b) a substrate functionalized with biotin–casein. The bar length is 10 μm.

for the extension force shows that the product $\varepsilon \cdot b$ should remain constant when b is varying. Experimentally, we have investigated about 20 cells for two different widths, namely 5 and 6.5 μm. Fractional extensions were found to be respectively 0.35 ± 0.3 and 0.27 ± 0.3, which indeed gives $\varepsilon \cdot b = 1.78 \pm 0.2$ and 1.76 ± 0.2. An estimate for the adhesion energy density w can then be derived: $w = 5\ \mu\text{J m}^{-2}$. By comparison, reported values for the adhesion energy of the streptavidin–biotin complex range from 100 μJ m^{-2} to a few nJ m^{-2} [23, 24]. However, the most accepted value for tight adhesion between biotinylated membrane and streptavidin-coated substrate is about 10 μJ m^{-2}, as obtained by Alberdorfer *et al* [25], which is in good agreement with our crude estimation.

3.3. Lipid vesicles as synthetic mimics of cells?

Over the last two decades giant vesicles have been extensively studied because of their potential relevance as minimal models for living cells. To date, the most refined design, which has been developed by Sackmann's group in Münich, contains three key ingredients: (1) the lipid bilayer; (2) the receptor–ligand pairs and (3) a PEG polymer brush. The aim of the present section is to study how such decorated giant vesicles behave on substrates bearing specific stickers.

More precisely, we have considered EPC vesicles doped with 4.5% lipid-PEG and 0.5% lipid-PEG-biotin. The molar fraction of lipid-PEG-biotin leads approximately to a surface coverage of 10% in streptavidin. The selected substrates are those used in the previous section. Figure 4 displays side-view images of a streptavidin vesicle on a surface passivated with casein (figure 4(a)) or activated with biotin–casein (figure 4(b)). Similar results were obtained with methoxy-PEG and biotin-PEG, respectively (not shown). The osmotically swollen vesicle was perfectly spherical with a contact angle lower than $10^\circ \pm 6^\circ$ when no biotin was present on the surface, which is indicative of the absence of significant non-specific interaction between the vesicle and the substrate. By contrast, in the presence of biotin, the shape of the vesicle was a truncated sphere, characterized by an extended adhesion patch and a contact angle of $45^\circ \pm 7^\circ$, which suggests that specific recognition is strongly promoted [25].

In order to show the firm character of adhesion of lipid-PEG-biotin vesicles, they were submitted to a linear shear flow (shear rate of 14.5 s^{-1}). Vesicles settled on the passive substrate started to slide and roll along the flow direction. Vesicles settled on the activated biotin–casein remained stuck in the same place. However, due to the shear stress, their membranes exhibited a rotating motion. Such vesicle spinning motion is clearly shown through the observation, on one vesicle, of a small defect, which is either trapped within the membrane lipid bilayer or simply bound to its internal part. It is illustrated in figure 5, where the defect is located in a vertical plane perpendicular to the axis of rotation, and slightly distant from the in-focus equatorial

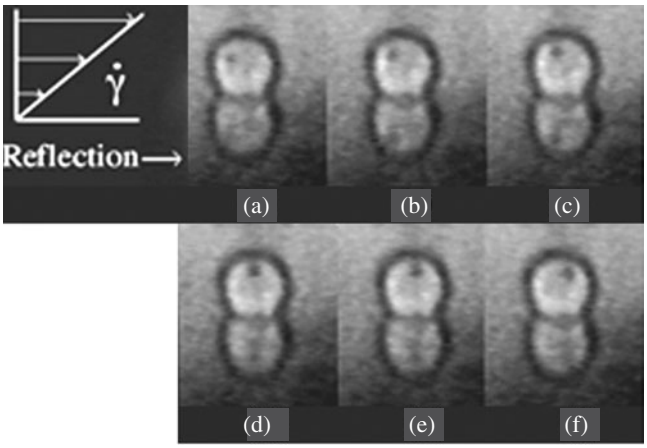

Figure 5. Spinning of a streptavidin-decorated vesicle subjected to a linear shear flow on a biotin–casein substrate. Vesicle radius: 7 μm. Shear rate $\dot{\gamma} = 14.5\ s^{-1}$. The vesicle remains at the same place but the membrane is rotating, as seen by the motion of a lipid defect (in black). (a) = 7 s, (b) = 7.2 s, (c) = 7.4 s, (d) = 7.6 s, (e) = 7.8 s, (f) = 8 s.

plane. This result strongly suggests that the membranar lipids, which are not involved in adhesion, can flow around the bounded biotin-PEG lipids located in the firm-adhesion contact zone. It reveals a specific adhesion behaviour, which requires fluid lipid membranes with mobile receptor sites.

The next step was to expose the same vesicles to micropatterned surfaces. Our interest was to visualize how the vesicle would spread and deform when intimate contact is only 'authorized' along a segment of line, which is narrow in comparison with the size of the vesicle. Quite surprisingly, as shown in figure 6(a), the RICM pattern of a vesicle at the corner of a step-like stripe does not exhibit exclusive adhesion along the biotinylated line. The vesicle seems to overflow the biotinylated stripe and be pushed against the supposedly passive surface. However, simultaneous visualization by fluorescence microscopy of the vesicle decorated with fluorescent streptavidin in the vicinity of the surface allowed us to better understand the actual situation. As shown in figure 6(b), only the biotinylated line became strongly fluorescent upon vesicle adhesion. In particular, the area circled in figure 6(a) was not fluorescent although close contact was observed by RICM. This means that, in spite of partial non-specific interaction, streptavidin molecules are only concentrated towards the biotin-derivatized area. The question which immediately arises is: why are vesicles, unlike red blood cells, not able to resist partial non-specific interaction when spreading is initiated by localized specific binding? Two explanations might be put forward. First, a vesicle decorated with PEG and ligands obviously lacks an inner cytoskeletal structure, which serves to provide higher rigidity of the membrane. For example, the bending modulus of an erythrocyte is $50k_BT$, i.e. five times as large as for an EPC vesicle [26]. Second, part of the glycocalix is anchored to the cytoskeleton in a real cell, while the PEG brush is mobile at the surface of vesicles. In particular, a forced approach between the mimetic membrane and the substrate is likely to cause depletion in PEG-lipids, which are expelled out of the contact area due to an excess of bidimensional osmotic pressure due to the polymer chains [12]. In contrast, the reduced mobility of glycopolymers may provide an additional kinetic barrier against depletion effects.

In a last set of experiments, we aimed to compare the spreading kinetics of streptavidin-coated vesicles and erythrocytes onto homogeneous biotinylated substrates. Individual settling

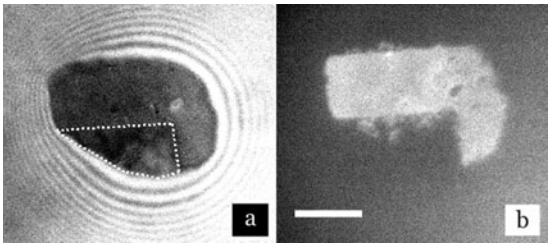

Figure 6. Adhesion of a giant vesicle decorated with fluorescent streptavidin on a biotinylated micropatterned surface. (a) RICM image; (b) fluorescence image. The dotted line in micrograph (a) shows the area of non-specific adhesion. The bar length is 5 μm.

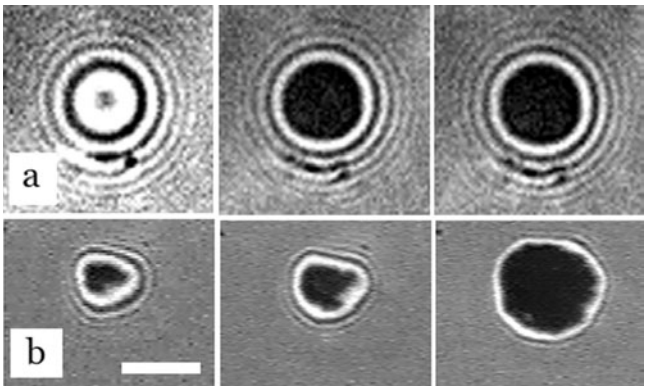

Figure 7. Time sequence of the spreading of (a) a streptavidin-decorated vesicle and (b) a streptavidin-derivatized red blood cell on a biotinylated surface as seen by RICM. Images are successively taken at t_0, $t_0 + 5$ s and $t_0 + 40$ s in both cases. The bar represents 5 μm.

vesicles or cells were first found by fluorescence microscopy before switching to RICM mode in order to monitor the spreading process. Figure 7(a) (respectively figure 7(b)) displays three snapshots taken at successive times (t_0, $t_0 + 5$ s, $t_0 + 40$ s) of a streptavidin-coated vesicle (respectively erythrocyte) spreading on a PEG-biotin substrate. Since vesicles and cells were osmotically swollen, single adhesion nuclei were usually observed close to the centre of the cell and were found to grow isotropically. Besides, by tuning the biotinylation time of red blood cells, we ensured that cells and vesicles were decorated with similar surface densities in streptavidin. As measured by fluorescence microscopy after calibration with vesicles containing various fractions of biotin-PEG-lipids (data not shown), the estimated streptavidin density was found to be equal to 5×10^{14} m^{-2}. Typical time evolution of the radius of contact (normalized by the radius of the vesicle or cell) is displayed in figure 8 (log–log plot) for both a vesicle and an erythrocyte. Immediately, we remark that the characteristic time for reaching the equilibrium shape is of the same order of magnitude ($\sim$50 s). However, the kinetics is completely different. For the red blood cell, the adhesion patch grows slowly at first, and after a few seconds, accelerates and roughly increases as $t^{0.7\pm0.06}$. For the vesicle, nucleation of the adhesion patch is followed by a rapid increase of the contact radius during the first second. In a second regime, a significant slowing down of the spreading kinetics is observed, since the patch grows as $t^{0.25\pm0.04}$. Despite the extensive theoretical work on equilibrium shapes of vesicles (see [25] and references therein), the dynamic aspect of spreading had been overlooked for a long time and recent theoretical studies are still tentative and controversial [27, 28]. Our

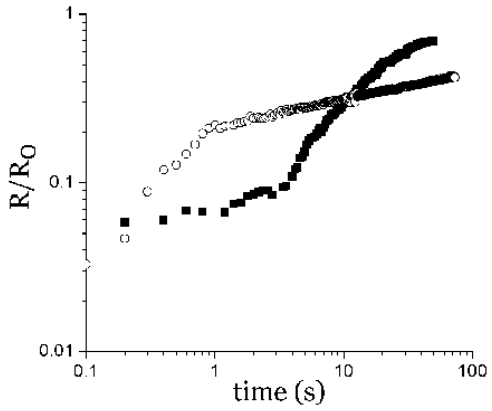

Figure 8. Typical time evolution of the radius of the adhesion patch normalized by the radius of the streptavidin-coated cell or vesicle for an erythrocyte (full squares) and for a vesicle (open circles) in a log–log scale.

goal is therefore not to propose an explanation for the observed growth laws. However, we believe it important to point out that, even though the statics of cell adhesion can be reasonably well emulated by properly decorated synthetic vesicles, the same vesicles fail in emulating the adhesion dynamics of cells as simple as erythrocytes. Of course, we had deliberately chosen to exclude more complex cells which are known to give rise to a large variety of adhesion patterns (fibrillar or focal points) induced by subtle reorganization of the cytoskeleton [29].

4. Conclusion

The aim of this paper was to discuss some difficulties related to the design of functionalized substrates and artificial cells for bioadhesion studies. We have tried to show that the biomimetic relevance of surface chemistry and membrane decoration strategies have to be tested in a cellular context. For example, specific molecular recognition does not preclude any non-specific adhesion of cells. We have proposed a simple method based on the use of functionalized PEG or casein which meets these basic requirements. From our viewpoint, the best up-to-date model for an artificial test cell seems to be the one in which a giant vesicle is doped with lipids bearing a headgroup modified with the ligand of interest and with PEG-lipids in order to mimic the repulsive activity of the glycocalix. Adhesive patterns of decorated liposomes on biomimetic surfaces are mostly similar to the behaviour of decorated erythrocytes. However, the spreading dynamics was found to be significantly different, which suggests that some relevant ingredients might be missing to achieve reliable biomimicry. More recent attempts to fill vesicles with actin filaments (in order to model the cytoskeleton) could be promising for the next generation of artificial cells and help in gaining insight into the physical basis of cell adhesion [30].

Acknowledgments

This work was supported by HFSP research grant 52/2003. We also received generous help from the Institut Curie. Part of this work was performed in the UMR 168 microfabrication room.

References

[1] Bell G J, Dembo M and Bongrand P 1984 *Biophys. J.* **45** 1051–64
[2] Bausch A R, Ziemann F, Boulbitch A A, Jacobson K and Sackmann E 1998 *Biophys. J.* **75** 2038–49
[3] Hermanson G T, Krishna Mallia A and Smith P K 1992 *Immobilized Affinity Ligand Techniques* (New York: Academic)
[4] Sackmann E 1996 *Science* **271** 43–8
[5] Ramsden J J 1998 *Biopolymers at Interfaces* (New York: Dekker)
[6] Mrksich M 1998 *Cell. Mol. Life Sci.* **54** 653–62
[7] Tanaka M and Sackmann E 2000 *TIBTECH* **18** 58–64
[8] Merkel R, Nassoy P, Leung A, Ritchie K and Evans E 1999 *Nature* **397** 50–3
[9] Cuvelier D, Rossier O, Bassereau P and Nassoy P 2003 *Eur. Biophys. J.* **32** 342–54
[10] Xia Y and Whitesides G M 1998 *Angew. Chem. Int. Edn* **37** 550–75
[11] Dimitrov D S and Angelova M I 1988 *Bioelectrochem. Bioenerg.* **19** 323–36
[12] Bruinsma R and Sackmann E 2001 *C. R. Acad. Sci.* IV **2** 803–15
[13] Rädler J and Sackmann E 1993 *J. Physique* II **3** 727–48
[14] Abkarian M, Lartigue C and Viallat A 2002 *Phys. Rev. Lett.* **88** 068103
[15] Weikl T R, Andelman D, Komura S and Lipowsky R 2002 *Eur. Phys. J.* E **8** 59–66
[16] Mooney J F, Hunt A J, McIntosh J R, Liberko C A, Walba D M and Rogers C T 1996 *Proc. Natl Acad. Sci. USA* **93** 12287–91
[17] Nelson K E, Gamble L, Jung L S, Boeckl M S, Naeemi E, Golledge S L, Sasaki T, Castner D G, Campbell C T and Stayton P S 2001 *Langmuir* **17** 2807–16
[18] Patel N, Sanders G H W, Shakesheff K M, Cannizzaro S M, Davies M C, Langer R, Roberts C J, Tendler S J B and Williams P W 1999 *Langmuir* **15** 7252–7
[19] Ryan P L, Foty R A, Kohn J and Steinberg M S 2001 *Proc. Natl Acad. Sci. USA* **98** 4323–7
[20] De Gennes P-G, Brochard-Wyart F and Quéré D 2002 *Gouttes, Bulles, Perles et Ondes (Berlin)*
[21] Parker K H and Winlove C P 1999 *Biophys. J.* **77** 3096–107
[22] Sleep J, Wilson D, Simmons R and Gratzer W 1999 *Biophys. J.* **77** 3085–95
[23] Moy V T, Jiao Y, Hillmann T, Lehmann H and Sano T 1999 *Biophys. J.* **76** 1632–8
[24] Albersdörfer A, Feder T and Sackmann E 1997 *Biophys. J.* **73** 245–57
[25] Tordeux C, Fournier J-B and Galatola P 2002 *Phys. Rev.* E **65** 041912
[26] Needham D and Zhelev D V 1996 *Surfactant Sci. Ser.* **62** 373–444
[27] Boulbitch A, Guttenberg Z and Sackmann E 2001 *Biophys. J.* **81** 2743–51
[28] De Gennes P-G, Puech P-H and Brochard-Wyart F 2003 *Langmuir* **19** 7112–9
[29] Kirchner J, Kam Z, Tzur G, Bershadsky A D and Geiger B 2003 *J. Cell Sci.* **116** 975–86
[30] Limozin L and Sackmann E 2002 *Phys. Rev. Lett.* **82** 168103